nature materials

LETTERS

PUBLISHED ONLINE: 16 SEPTEMBER 2012 | DOI: 10.1038/NMAT3408

Heterogeneous nucleation of organic crystals mediated by single-molecule templates

Koji Harano[1], Tatsuya Homma[1], Yoshiko Niimi[2], Masanori Koshino[2], Kazu Suenaga[2], Ludwik Leibler[3] and Eiichi Nakamura[1]*

Fundamental understanding of how crystals of organic molecules nucleate on a surface remains limited[1–3] because of the difficulty of probing rare events at the molecular scale. Here we show that single-molecule templates on the surface of carbon nanohorns can nucleate the crystallization of two organic compounds from a supersaturated solution by mediating the formation of disordered and mobile molecular nanoclusters on the templates. Single-molecule real-time transmission electron microscopy indicates that each nanocluster consists of a maximum of approximately 15 molecules, that there are fewer nanoclusters than crystals in solution, and that in the absence of templates physisorption, but not crystal formation, occurs. Our findings suggest that template-induced heterogeneous nucleation mechanistically resembles two-step homogeneous nucleation[4–7].

Observations and studies of heterogeneous nucleation on the molecular scale have been challenging. Here we conceived a synthetic method to prepare a substrate bearing single-molecule templates and perform their analysis with the aid of the single-molecule real-time transmission electron microscopy (SMRT-TEM) imaging technique[8,9]. Of particular importance was the proper choice of the substrate. A sea-urchin-like aggregated particle of carbon nanohorns[10] bearing amine groups (amino–CNHs, Fig. 1a, top left; Fig. 1b) was the substrate of choice for several reasons[11]. The CNH particle is a water-soluble macromolecule, which has an approximate molecular formula of $C_{70,000,000}N_{100,000}H_{200,000}$–$C_{170,000,000}N_{300,000}H_{600,000}$ with an average molecular weight of 8–20 × 10^8 Da and a diameter of 50–150 nm, consisting of about 2,000 individual nanohorns (spikes)[12]. It has a graphite surface, on which many NH_2 groups are located, primarily at two peripheral sites: the end cap of a CNH spike and the structural defects on its sidewall. These NH_2 groups can be readily derivatized by amide bond formation[12]. The CNH particles are chromatographically purifiable and can be isolated by filtration. Most importantly, the particles are hollow and allow TEM imaging of single organic molecules and molecular clusters attached to the surface of the solid[13]. Note that neither ordinary carbon nanotubes nor common organic and inorganic nanoparticles have the above properties required in the present study.

We chose the C_3-tribromide Y as the compound to be crystallized, which serves the purpose of the present study because the bromine atoms facilitate structural analysis by SMRT-TEM and the crystal does not contain any solvent molecules[14]. A unit cell of the crystal contains 12 molecules, consisting of four sets of three molecules stacked by both π–π and CH–π interactions through twisting of the three benzene rings (Supplementary Fig. S1).

For crystallization of Y, we designed a molecular template Y′ on CNH (Y′–CNH), where a C_s-symmetric molecule Y′ is bonded to amino–CNH through a structurally inflexible amide bond so that the molecule stands upright without touching the CNH surface (see Fig. 2a,b). We synthesized Y′–CNH by acylation of amino–CNH with Y′–imide (see Fig. 1a) in 50% aqueous *N*,*N*-dimethylformamide (DMF). Such acylation of amino–CNH was previously shown to take place with several % yield[12], putting a few molecules of Y′-template for each CNH or about 6,000 Y′ on one CNH particle, as we confirmed here by SMRT-TEM. Y′–CNH was isolated by filtration and washed with DMF to remove excess Y′–imide. SMRT-TEM analysis showed that Y′ molecules indeed stand upright on the CNH surface, and remain flexible to undergo stochastically conformational change several times per minute (Fig. 2a,b and Supplementary Movie S1)[15]. The observed conformational change seems to be due largely to the rotation of the central biphenyl moiety.

We then performed a series of macroscopic crystallization experiments in the absence and presence of Y′–CNH, and compared the amounts of isolated needle crystals. First, we crystallized 2.78 mg of Y by itself in a 2.00 ml dust-free supersaturated EtOH solution from 70.0±0.1 °C gradually cooled (10 °C h^{-1}) to 25.0±0.1 °C over 72 h, and obtained 0.34 mg of long needle crystals (Fig. 3a, leftmost column; Y′/Y = 0; average length = 871±35 μm with an aspect ratio of 1:10 to 1:50). Then, we crystallized the same amount of Y in the presence of the Y′–CNH particles (0.055 mg, mole ratio Y′/Y = 1.2×10^{-4}, Fig. 3a, second left column), and obtained crystals of Y (about 0.84 mg) whose average length was shorter (280±15 μm; Fig. 3a, inset). We found roughly 10^4–10^6 crystals larger than about 10 μm (each crystal is estimated to contain very roughly 10^{12}–10^{14} Y molecules). When we increased the amount of Y′–CNH by a factor of 10 (Y′/Y = 1.2×10^{-3}, 0.55 mg), the crystal length became shorter, as expected (Fig. 3a, inset). A further increase by another factor of 10 (Y′/Y = 1.2×10^{-2}, 5.50 mg for 2.78 mg of Y) resulted in extensive adsorption (Fig. 3a, rightmost column)[13].

We found numerous Y′–CNH particles attached to the surface of the template-grown crystals (Fig. 1c,d), whereas the Y′–CNH particles were rarely found attached to the crystals when we added the particles after the completion of crystallization (Supplementary Fig. S4). This indicates that one Y′–CNH particle causing nucleation becomes incorporated in the crystal, and many more CNH particles may also do so during the crystal growth.

Control experiments indicated that neither the Y′ group nor the CNH can promote crystallization. Thus, crystallization in the presence of the Y′–imide molecule (that is, without CNHs) (Y′/Y = 1.2×10^{-3}) gave essentially the same size and weight of

[1]Department of Chemistry, The University of Tokyo, Hongo, Bunkyo-ku, Tokyo 113-0033, Japan, [2]Nanotube Research Centre, National Institute of Advanced Industrial Science and Technology (AIST), Tsukuba 305-8565, Japan, [3]The Soft Matter and Chemistry Laboratory UMR 7167, École supérieure de physique et de chimie industrielles de la ville de Paris, 10 rue Vauquelin 75005 Paris, France. *e-mail: nakamura@chem.s.u-tokyo.ac.jp.

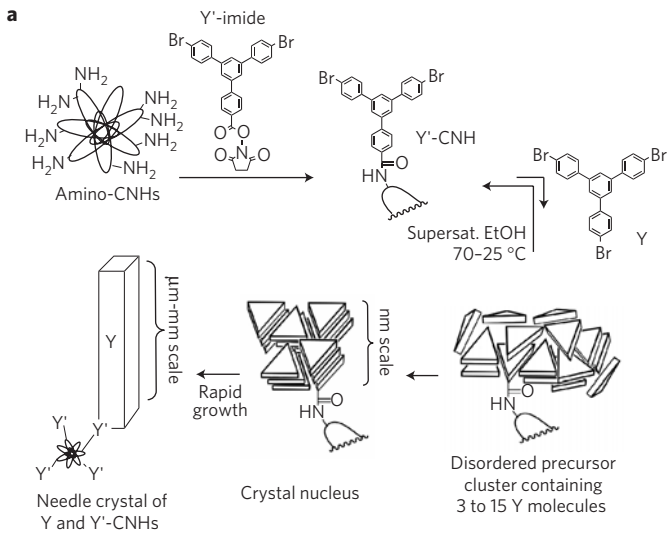

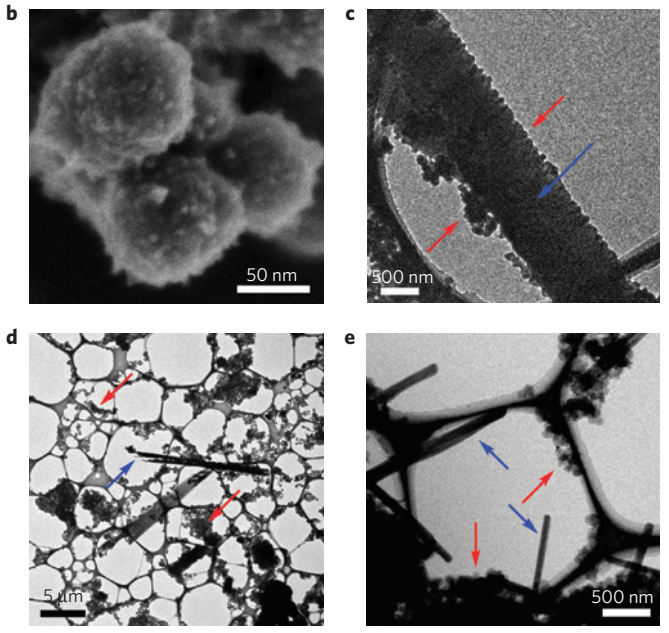

Figure 1 | Y′–CNH-driven crystallization of 1,3,5-tris(4-bromophenyl) benzene (Y). a, Schematic illustration of experiments. **b**, SEM image of Y′–CNH particles. **c**, TEM image of a needle crystal (blue arrow), to the surface of which Y′–CNH particles are densely attached (red arrows). The sample was taken from the crystallization solution using 1.2×10^{-3} equiv. of Y′–CNH. **d**, TEM image of the same sample, where we find several crystals (blue arrow) and numerous Y′–CNH particles (red arrows). **e**, Scanning transmission electron microscopic (STEM) image of small needle crystals (blue arrows) grown in the presence of amino–CNH particles (red arrows), indicating that no amino–CNH particles are attached to the crystal surface (see **c**).

crystals as those without Y′–CNH (that is, crystallization of Y alone; data not shown). Moreover, crystallization in the presence of amino–CNH (0.55 mg; that is, without Y′) afforded only a tiny amount of <1-μm-sized crystals to which no CNH particles were attached (Fig. 1e). Scanning electron microscopy (SEM)-energy-dispersive X-ray spectroscopic analysis of the recovered amino–CNH showed that amino–CNH had strongly adsorbed Y molecules on its surface (Supplementary Fig. S5). Note that the same 0.55-mg quantity of Y′–CNH induced the formation of a large amount of crystals (Fig. 3a) while it also strongly adsorbed Y on its surface (Fig. 2d, green arrow).

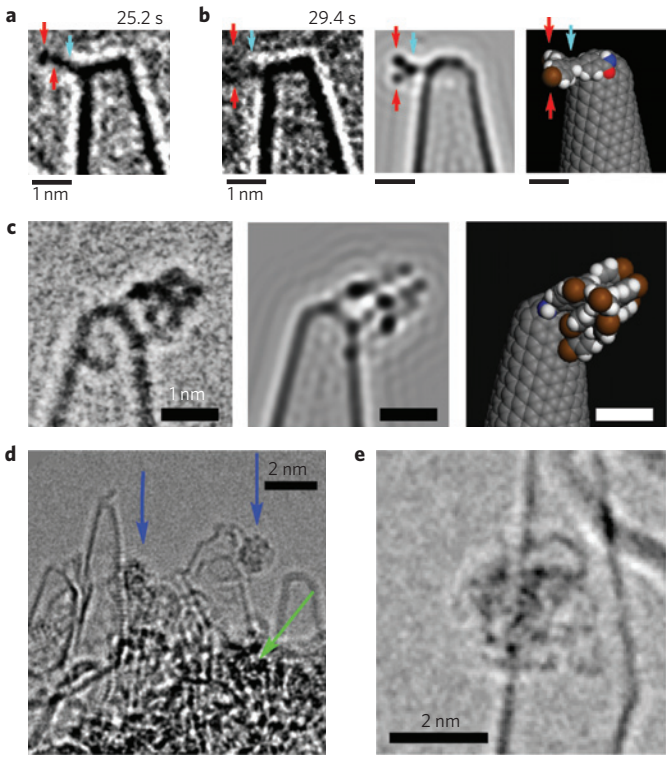

Figure 2 | SMRT-TEM images of Y′–CNH and precursor clusters of Y taken from the Supplementary Movies together with a molecular model of a plausible structure of clusters and its TEM simulation. a, TEM image of Y′ on a CNH. The figure captions refer to the time (s) after initiation of the observation (see Supplementary Movie S1). Red arrows and a light-blue arrow indicate the bromophenyl and the central benzene groups, respectively. **b**, TEM image of the same Y′ in **a** on the left, a model on the right, and the TEM simulation in the middle. Details of the molecular modelling and the TEM simulation are described in Supplementary Section S1. See the movie for another Y′ molecule (Supplementary Movie S2), in which the bromophenyl groups are more visible because of the more restricted motion. Arrow indications are the same as for **a**. **c**, TEM image of a termolecular cluster made of two Y on one Y′, a model on the right and the simulation in the middle. To reproduce the experimental TEM image, it was essential to have both π–π and CH–π intermolecular interactions, as found in a single crystal of Y. **d**, TEM image of several Y′–CNHs with two large spherical clusters of Y (blue arrows) and many Y molecules (green arrow) adsorbed in the CNH grooves (bottom). **e**, TEM image of a large disordered cluster composed of about 15 molecules, the core of which is surrounded by an amorphous boundary layer shown as curved lines. All TEM images were taken on an instrument operating at 293 K (120 kV, 2.3 Å resolution, 1×10^{-5} Pa) or one operating at 4 K (80 kV, 2.3 Å resolution, 1×10^{-5} Pa; see details in Supplementary Section S1) with a 0.5-s imaging time (electron irradiation of 3.6×10^{4} e^{-} nm^{-2} for one frame) followed by a 1.6-s charge-coupled device data read-out time (no irradiation) for a total observation time of at least a few minutes (total dose of about 2.0×10^{6} e^{-} nm^{-2}).

We next retrieved by quick filtration the Y′–CNH particles used for seeding, and analysed them by *ex situ* SMRT-TEM imaging, finding two types of mobile molecular aggregate in the crystallized mixture: nanometre-sized mobile molecular clusters that slowly rotate and change their shape under TEM imaging (Fig. 2c) and micrometre- to millimetre-sized needle crystals. No objects of intermediate sizes were found. Twenty of the nanometre-sized clusters examined were situated in locations suitable for structural analysis in some detail. The structure of the smallest one was determined at a high confidence level to be a termolecular van

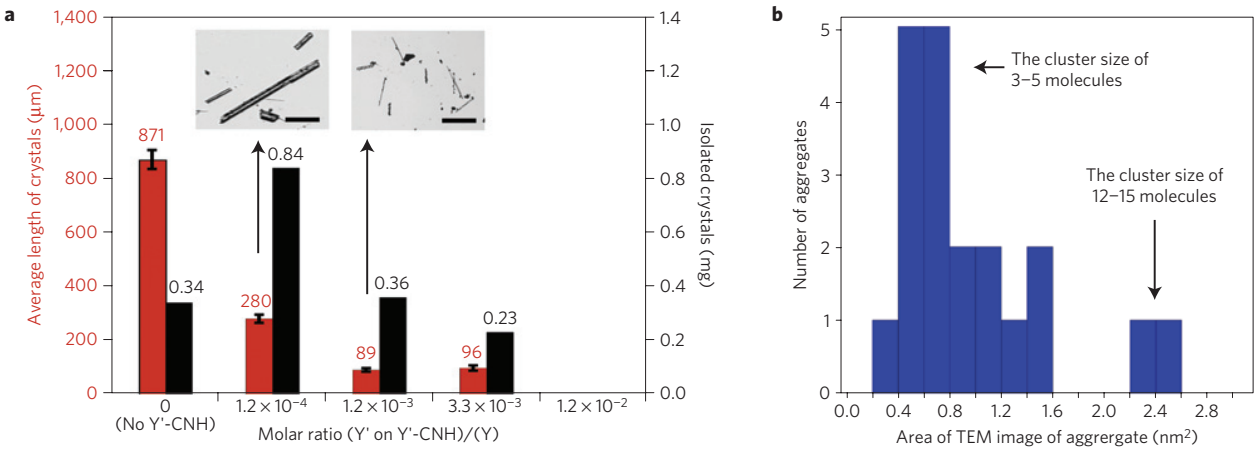

Figure 3 | Size of needle crystals and clusters of Y on Y′–CNH. a, Length and weight of needle crystals of Y plotted against the mole ratio of Y′ in CNH and Y. Optical microscopic images of the crystals in the insets (scale bar: 100 μm). Red and black numbers over bars indicate average length and weight, respectively. Error bars show standard errors of the mean. **b**, Histogram of the number of Y clusters (total 20) plotted against the area of TEM images simulated by rectangles (studied for the sample with $Y'/Y = 1.2 \times 10^{-3}$). We found neither clusters nor crystals with sizes larger than Y′ + 15Y clusters and smaller than micrometre-sized needle crystals.

der Waals cluster, as shown in Fig. 2c. Larger clusters are spherical (see Fig. 2d,e), and the largest one found was composed of about 15 molecules, with about 10 molecules forming a disordered core and several covering the core as a unimolecular-thick film (Fig. 2e). This image lends experimental support to a proposed structure of precursor clusters[5,7,16–19].

The size distribution of the nanometre-sized van der Waals clusters shown in Fig. 3b is consistent with the energetics of crystal growth proposed by Gibbs[20]. This graph suggests that the critical cluster size in the present system is about 15 molecules, and is close to those previously suggested for crystallization of proteins and polymers (20–160; refs 21–23).

Because we can count the number of clusters as well as Y′-templates on one CNH particle (see above), we estimated the ratio between the templates and the clusters to be approximately 300:1. Using the average molecular weight and the weight of amino–CNH as well as the approximate number of micrometre-sized crystals formed, we estimate the ratio between the Y′-template, the cluster, and the large crystal to be $(2 \times 10^9–5 \times 10^{11}):(6 \times 10^6–2 \times 10^9):1$, when $Y'/Y = 6.0 \times 10^{-3}$ (see details in Supplementary Section S1). On the basis of such a large value for the cluster/crystal ratio and the absence of ordered clusters (that is, crystalline nuclei) among clusters we examined by SMRT-TEM (ref. 24), we consider that the probability of conversion of a disordered cluster to a crystalline nucleus within a specified time depends on such factors as the conformational and orientational mobility of the molecules, van der Waals and solvophobic forces exerted on the cluster, and temperature[25]. Once a correct molecular ordering is obtained for at least one cluster in solution, rapid growth of this cluster starts and depletes the molecules from the supersaturated solution.

We also show that Y′–CNH can nucleate two similar but different types of molecules, that is, C_s-symmetric compound Y′-imide and C_3-symmetric compound Y (Fig. 4a). Thus, when the amino–CNH particles and Y′–imide were mixed at 70 °C and cooled to room temperature in 50% aqueous EtOH, we found many disordered clusters of Y′–imide (Fig. 4b and Supplementary Movie S7) in addition to the formation of Y′–CNHs. This observation also provides an indication of how a reactive surface *in situ* forms single-molecule nucleation sites and promotes nucleation (Fig. 4c).

Finally, we emphasize the mildness of the SMRT-TEM imaging technique by pointing out that even van der Waals molecular clusters did not decompose up to a total electron dose of 2.0×10^6 e^- nm^{-2} (imaging for several minutes at a 120-kV acceleration voltage)[26], and that the motions of Y′ molecules have very low frequency (only 4–10 bond rotation motions per minute on either a 4 K or a 293 K sample stage; Fig. 2a,b and the corresponding Supplementary Movie S1–S3, showing another molecule of Y′ on CNH)[27]. The movies also illustrate the unique ability of SMRT-TEM to allow the analysis of a mixture of molecules and molecular clusters without purification. Molecular science rarely has the opportunity to consider and visualize the fate of an individual small molecule in a fluid. The observation of the precursor clusters demonstrates the ability of the atomic resolution SMRT-TEM imaging to provide such an unusual insight, and also suggests its utility in the studies of nucleation and crystallization.

In summary, the SMRT-TEM imaging experiments have provided several important insights into the elusive mechanism of heterogeneous nucleation not previously addressed by macroscopic studies. First, a single-molecule template connected to the surface of a solid can nucleate crystals through formation of nanometre-sized molecular clusters, which consist of no more than 15 molecules, as determined *ex situ* by SMRT-TEM. We also found that the molecular template formed *in situ* on an activated surface can nucleate crystallization. Second, we estimated that only one out of 10^9–10^{11} templates becomes incorporated into a large crystal (see Supplementary Section S1), indicating that nucleation from a single template occurs with an extremely small probability and that only a small number of rapidly growing crystalline nuclei deplete the molecules from the solution. Third, the molecular clusters are structurally mobile and disordered, and we could not find any structurally ordered crystalline nuclei, suggesting that crystalline nuclei grow into large crystals as soon as they form. These results agree with the energetics proposed by Gibbs[20], and suggest that the mechanism of heterogeneous nucleation resembles the two-step mechanism of homogeneous nucleation[4–7]. Fourth, we made an intriguing observation that one template can nucleate two different molecules. Apparently, one template molecule in a cluster can induce the periodicity of a crystal out of many fluctuating molecules in the critical cluster within a finite period of time, and the same template can do so for another similar but different type of molecule. This mechanism of heterogeneous nucleation is conceptually different from those proposed previously[1,2]. We also found that physisorption on CNHs hampers crystal formation rather than promotes it, which we consider rather reasonable because the conformation of 3D crystals of Y molecules differs from that of 2D crystals formed on a graphite surface[28]. We expect that

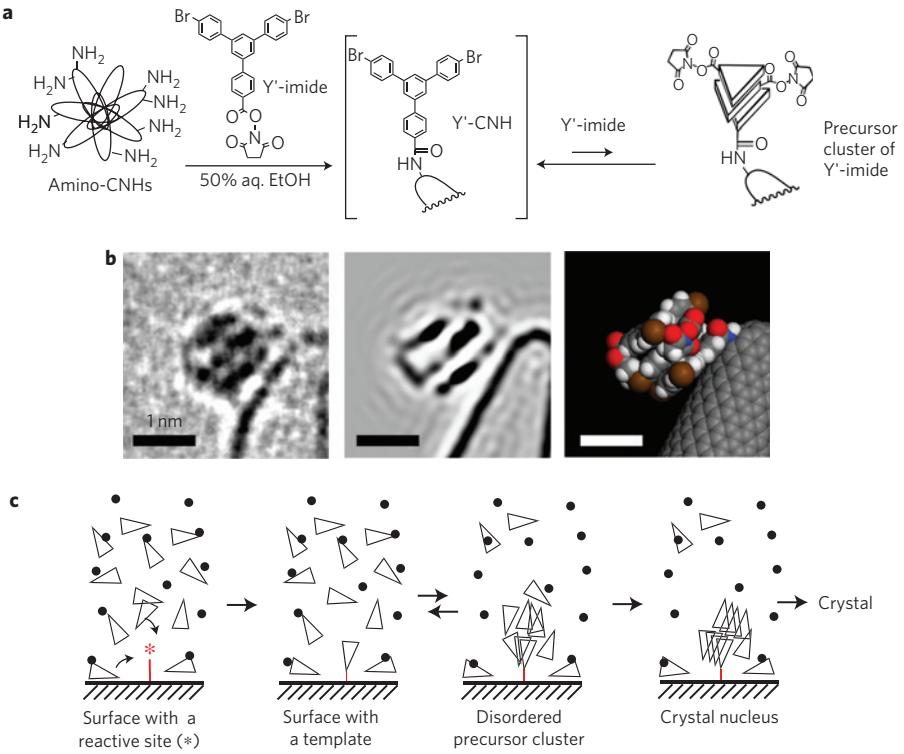

Figure 4 | Nucleation on a reactive surface. a, *In situ* formation of Y′–CNH and a precursor cluster of Y′–imide on amino-CNH. **b**, TEM image of two Y′–imide molecules and Y′ on the left, the model on the right and the simulation in the middle. **c**, Nucleation on a reactive surface. A reactive surface chemically traps a molecule, which then acts as a template to form a disordered precursor cluster, a crystal nucleus, and a crystal. Some molecules may be adsorbed on the surface or form 2D crystals, but cannot form 3D crystals because 2D and 3D crystals require different molecular conformations and orientations. Triangles: crystallizing molecules; dots: solvent molecules; red star: reactive species on the surface capturing a crystallizing molecule.

SMRT-TEM imaging will allow us to obtain further insights into the crystallization and phase-segregation phenomena frequently encountered in materials science research[29], and will be useful for those engaged in the analysis and design of such processes[30].

Methods

Crystallization of Y in the presence of Y′–CNH. A typical crystallization experiment of $Y'/Y = 1.2 \times 10^{-4}$ is described. Y′–CNH (0.055 mg, 0.61 nmol of Y′) was mixed with an EtOH solution (2 ml, filtered through a PTFE membrane filter, pore size: 200 nm, just before use) of Y (2.78 mg, 5.12 μmol) at 70 °C in a glass vial, and the two-phase suspension was sonicated for 1 min to obtain a homogeneous mixture of Y′–CNH and Y in EtOH. The vial was placed in a temperature-controlled incubator at 70.0 ± 0.1 °C. The mixture was gradually cooled (10 °C h^{-1}) to 25.0 ± 0.1 °C during 4.5 h. After 72 h, the mixture was filtered through a PTFE membrane filter (pore size: 200 nm), washed rapidly with EtOH (1 ml, in which the crystals are scarcely soluble at 25 °C) and then dried in vacuo for 12 h to obtain a mixture of black powder and colourless needle crystals (0.90 mg in total).

Preparation of a sample for SMRT-TEM observation. The black powder of the carbon nanohorn (about 1 mg) was dispersed in MeOH (10 ml) by bath sonication (2 s × 5). A droplet of the suspension was placed onto a TEM mesh precoated by microgrids. Excess solvent was blotted by a filter paper, and then the TEM mesh was dried under reduced pressure (6×10^{-4} Pa) for 1 h before observation by SMRT-TEM.

Received 9 February 2012; accepted 25 July 2012; published online 16 September 2012

References

1. Markov, I. V. *Crystal Growth for Beginners* 2nd edn (World Scientific, 2002).
2. Sear, R. P. Nucleation: Theory and applications to protein solutions and colloidal suspensions. *J. Phys. Condens. Matter* **19,** 033101 (2007).
3. Sommerdijk, N. A. J. M. & de With, G. Biomimetic $CaCO_3$ mineralization using designer molecules and interfaces. *Chem. Rev.* **108,** 4499–4550 (2008).
4. Ten Wolde, P. R. & Frenkel, D. Enhancement of protein crystal nucleation by critical density fluctuations. *Science* **277,** 1975–1978 (1997).
5. Vekilov, P. G. Dense liquid precursor for the nucleation of ordered solid phases from solution. *Cryst. Growth Des.* **4,** 671–685 (2004).
6. Erdemir, D., Lee, A. Y. & Myerson, A. S. Nucleation of crystals from solution: Classical and two-step models. *Acc. Chem. Res.* **42,** 621–629 (2009).
7. Vekilov, P. G. Nucleation. *Cryst. Growth Des.* **10,** 5007–5019 (2010).
8. Koshino, M. *et al.* Imaging single molecules in motion. *Science* **316,** 853 (2007).
9. Nakamura, E. in *Chemistry of Nanocarbons* (eds Akasaka, T., Wudl, F. & Nagase, S.) 405–412 (Wiley-VCH, 2010).
10. Iijima, S. *et al.* Nano-aggregates of single-walled graphitic carbon nano-horns. *Chem. Phys. Lett.* **309,** 165–170 (1999).
11. Isobe, H. *et al.* Preparation, purification, characterization, and cytotoxicity assessment of water-soluble, transition-metal-free carbon nanotube aggregates. *Angew. Chem. Int. Ed.* **45,** 6676–6680 (2006).
12. Nakamura, E. *et al.* Imaging of conformational change of biotinylated triamide molecules covalently bonded to carbon nanotube surface. *J. Am. Chem. Soc.* **130,** 7808–7809 (2008).
13. Hashimoto, S. *et al.* Anomaly of CH_4 molecular assembly confined in single-wall carbon nanohorn spaces. *J. Am. Chem. Soc.* **133,** 2022–2024 (2011).
14. Beltran, L. M. C., Cui, C., Leung, D. H., Xu, J. & Hollander, F. J. 1,3,5-Tris(*p*-bromophenyl)benzene. *Acta Cryst.* **E58,** o782–o783 (2002).
15. Solin, N. *et al.* Imaging of aromatic amide molecules in motion. *Chem. Lett.* **36,** 1208–1209 (2007).
16. Trevius, E. B. Precrystallization state in salt aqueous solutions. *Crystallogr. Rep.* **46,** 1039–1045 (2001).
17. Lutsko, J. & Nicolis, G. Theoretical evidence for a dense fluid precursor to crystallization. *Phys. Rev. Lett.* **96,** 046102 (2006).
18. Chattopadhyay, S. *et al.* SAXS study of the nucleation of glycine crystals from a supersaturated solution. *Cryst. Growth Des.* **5,** 523–527 (2005).
19. Pouget, E. M. *et al.* The initial stages of template-controlled $CaCO_3$ formation revealed by cryo-TEM. *Science* **323,** 1455–1458 (2009).
20. Gibbs, J. W. On the equilibrium of heterogeneous substances. *Trans. Connect. Acad. Sci.* **3,** 108–248 (1876).
21. Yau, S-T. & Vekilov, P. G. Direct observation of nucleus structure and nucleation pathways in apoferritin crystallization. *J. Am. Chem. Soc.* **123,** 1080–1089 (2001).
22. Gasser, U., Weeks, E. R., Schofield, A., Pusey, P. N. & Weitz, D. A. Real-space imaging of nucleation and growth in colloidal crystallization. *Science* **292,** 258–262 (2001).

23. Jonkheijm, P., van der Schoot, P., Schenning, A. P. H. J. & Meijer, E. W. Probing the solvent-assisted nucleation pathway in chemical self-assembly. *Science* **313,** 80–83 (2006).
24. Guo, Y. *et al.* Ultrastable nanostructured polymer glass. *Nature Mater.* **11,** 337–343 (2012).
25. Filobelo, L. F., Galkin, O. & Vekilov, P. G. Spinodal for the solution-to-crystal phase transformation. *J. Chem. Phys.* **123,** 014904 (2005).
26. Nakamura, E. *et al.* Electron microscopic imaging of a single group 8 metal atom catalyzing C–C bond reorganization of fullerenes. *J. Am. Chem. Soc.* **133,** 14151–14153 (2011).
27. Koshino, M., Solin, N., Tanaka, T., Isobe, H. & Nakamura, E. Imaging of the passage of a single hydrocarbon chain through a nanopore. *Nature Nanotech.* **3,** 595–597 (2008).
28. Gutzler, R. *et al.* Surface mediated synthesis of 2D covalent organic frameworks: 1,3,5-Tris(4-bromophenyl)benzene on graphite(001), Cu(111), and Ag(110). *Chem. Commun.* 4456–4458 (2009).
29. Matsuo, Y. *et al.* Columnar structure in bulk heterojunction in solution-processable three-layered p-i-n organic photovoltaic devices using tetrabenzoporphyrin precursor and silylmethyl[60]fullerene. *J. Am. Chem. Soc.* **131,** 16048–16050 (2009).
30. Diao, Y., Myerson, A. S., Hatton, T. A. & Trout, B. L. Surface design for controlled crystallization: The role of surface chemistry and nanoscale pores in heterogeneous nucleation. *Langmuir* **27,** 5324–5334 (2011).

Acknowledgements

This work was partly supported by KAKENHI on Specially Promoted Research (22000008) to E.N. and Innovative Areas 'Coordination Programming' (Area 2107, 24108710) to K.H. from MEXT, Japan. T.H. thanks the Japan Society for Promotion of Science for a predoctoral fellowship. The CNH particles for the synthesis of amino–CNH were provided by M. Yudasaka.

Author contributions

E.N. conceived the study and co-wrote the paper with K.H. T.H. and K.H. performed the macro- and microscopic experiments and L.L. conceived the macroscopic experiments. M.K. and Y.N. performed the SMRT-TEM imaging, and interpreted the data with K.S., K.H., E.N. and T.H. All authors discussed the results and commented on the manuscript.

Additional information

Supplementary information is available in the online version of the paper. Reprints and permissions information is available online at www.nature.com/reprints. Correspondence and requests for materials should be addressed to E.N.

Competing financial interests

The authors declare no competing financial interests.